Physica Medica 97 (2022) 66–72

Contents lists available at ScienceDirect

Physica Medica

journal homepage: www.elsevier.com/locate/ejmp

Small static radiosurgery field dosimetry with small volume ionization chambers

Miguel López-Sánchez [a,e], María Pérez-Fernández [a], Eduardo Pardo [b], José M Fandiño [c], Antonio Teijeiro [d], Nicolás Gómez-Fernández [e], Faustino Gómez [e], Diego M González-Castaño [e,*]

[a] Hospital Universitario Lucus Augusti, R. Dr. Ulises Romero, 1, E-27003, Lugo, Spain
[b] Hospital Universitario Quirónsalud Madrid, C. Diego de Velázquez, 1, E-28223, Pozuelo de Alarcón, Spain
[c] Centro Oncológico de Galicia, Rúa Doctor Camilo Veiras, 1, E-15009, A Coruña, Spain
[d] Complexo Hospitalario Universitario de Vigo, Estrada do Meixoeiro, s/n, E-36214, Vigo, Spain
[e] Radiation Physics Laboratory, AII, University of Santiago de Compostela, E. San Lourenzo S/N, E-15705, Santiago de Compostela, Spain

ARTICLE INFO

Keywords:
IBA razor nano
Small field dosimetry
SRS
Monte Carlo simulation

ABSTRACT

Purpose: To evaluate the response of the four smallest active volume thimble type ionization chambers commercially available (IBA-dosimetry RAZOR Nano Chamber, Standard Imaging Exradin A16, IBA-dosimetry CC01 and PTW T31022) when measuring SRS cone collimated Flattening Filter Free (FFF) fields.
Methods: We employed Monte Carlo simulation for calculating correction factors as defined in IAEA TRS-483. Monte Carlo simulation beam model and ion chamber geometry definitions were supported by an extensive set of measurements. Type A and B uncertainty components were evaluated.
Results: Commissioning of Monte Carlo 6 MV and 10 MV FFF beam models yielded relative differences between measured and simulated dose distributions lower than 1.5%. Monte Carlo simulated output factors for 5 mm SRS field agree with experimental values within 1% local relative difference for all chambers. Smallest active volume ion chamber (IBA-dosimetry RAZOR Nano Chamber) exhibits smallest correction, being compatible with unity. Correction factor combined uncertainties range between 0.7% and 0.9%. Smallest uncertainties were recorded for smallest and largest active volume ion chambers, although the latter exhibited largest correction factor. Highest contribution to combined uncertainty was type B component associated with beam model initial electron spatial Full Width Half Maximum (FWHM) uncertainty.
Conclusions: Among the investigated chambers, the IBA RAZOR Nano Chamber was found to be an excellent choice for narrow beam output factor measurement since it requires minimum correction (in line with IAEA TRS-483 recommendations). This is caused by its tiny size and tissue equivalence materials which produce minimum volume averaging and fluence perturbation.

Introduction

Ion chambers have been used extensively in radiotherapy dosimetry [1]. Their advantages are robustness, stability, adequate tissue equivalence at therapy energy range, small recombination at conventional therapy dose per pulse rates and most of all an extensively and standardized theory describing corrections needed to calculate absorbed dose from their reading. With the increase of small field usage in radiotherapy, especially with the advent of Intensity Modulated Radiation Therapy (IMRT) and other techniques using Multi-Leaf Collimator (MLC), smaller active volume detectors were needed. Ion chamber main limitations show up when measuring beams narrower than 2 cm or at beam penumbra [2]. Due to air low sensitivity, active volumes are not usually constructed with sizes smaller than 2–3 mm. This produces volume averaging in small field dosimetry [3,4]. Chamber materials can also produce significant perturbation effects in these small fields [5]. Other limitations are polarity effect dependence on field size and other electric effects related to low signal to noise ratio such as stem/cable effect and signal instability [3,5,6]. Early small active volume chambers exhibited limited accuracy in these fields [2]. Early solid state detectors showed poor tissue equivalence and suffered important total ionizing dose damage. They also presented discrepancies of the detector response from equally manufactured dosimeters [7]. More recently, with the increased use of highly modulated fields or small fields such as those

* Corresponding author.

https://doi.org/10.1016/j.ejmp.2022.04.002
Received 25 October 2021; Received in revised form 15 March 2022; Accepted 9 April 2022
Available online 13 April 2022

used in Stereotactic Radiation Therapy (SRS) and Stereotactic Body Radiation Therapy (SBRT), chambers have been mostly replaced by solid state detectors such as synthetic diamond [8,9]. Latest developments in Radiotherapy may require new construction designs for both ion chambers and solid state detectors [10,11].

Small field dosimetry with solid state detectors has been extensively studied, especially with the recent synthetic diamond which has better tissue equivalence [8]. IAEA TRS-483 recommends using a detector requiring no correction for small field dosimetry [1]. Nevertheless, many works presenting correction factors for these solid state detectors have been published [12–15]. Results in these works show that simulations are sensitive to exact detector geometry, of which there might be a limited knowledge, leading sometimes to artificial results [13] which had to be reviewed afterwards [15,16]. Also, unit to unit detector differences exist due to manufacturing tolerances, which limits universality of published data [12,16]. Despite this, these synthetic diamonds have proven to be a suitable detector for small field dosimetry [17]. Recently small active volume ion chamber designs have been improved and now detectors with volumes as small as 0.003 cm^3 are available. This may render ion chambers appropriate again for state of the art small field dosimetry [18,19]. Existing bibliography is limited but shows the validity of this detector for small field dosimetry [19,20].

The aim of this work is to evaluate the response of these small active volume ion chambers when measuring small static fields, by calculating Monte Carlo correction factors supported by experimental verification. These correction factors can be used to correct measurements for the effects in chamber response associated with small field dosimetry (mainly volume averaging and lack of lateral electronic equilibrium) and/or to define the range of field sizes in which the correction is smaller than certain tolerance and therefore the un-corrected miss-response of the chamber is tolerable. In this study we focused on 6 MV and 10 MV FFF, 5 mm SRS fields dosimetry with four ion chambers with active volumes ranging between 0.003 and 0.016 cm^3. Accurate small field measurements are essential for a proper commissioning of Treatment Planning Systems devoted to SRS and SBRT or Highly Modulated radiotherapy where narrow beams are employed [21,22].

Methods

In this work we studied the response of ionization chambers when measuring small static FFF beams by calculating their correction factors associated with output factors, usually expressed as: $k^{f_{clin},f_{ref}}_{Q_{clin},Q}$. We calculated these factors by simulating by Monte Carlo the four absorbed doses in the following expression:

$$k^{f_{clin},f_{ref}}_{Q_{clin},Q} = \frac{\frac{D_{w,clinc}}{D_{w,ref}}}{\frac{D_{IC,clinc}}{D_{IC,ref}}} \quad (1)$$

Where $D_{w,clinic}$ and $D_{w,ref}$ are calculated absorbed doses to water within a small scoring water volume (voxel) placed at reference depth inside a water phantom for clinical and reference beams, respectively. $D_{IC,clinic}$ and $D_{IC,ref}$ are the absorbed dose to air within the cavity of an ionization chamber placed at same position as water voxels for clinical and reference beams, respectively. For obtaining beam models we used methods developed in a previous work and applied them to 6 MV FFF (6FFF) and to 10 MV FFF (10FFF) beams [23].

Evaluated chambers considered in this study are listed and described in the following table:

We also evaluated the response of smallest and largest active volume ion chambers along small field lateral and depth profiles. For this, we simulated beam profiles and Percentage Depth Dose (PDD) of the 5 mm cone using a small water voxel as reference scoring voxel and compared that to the simulated result. This comparison is presented as a correction factor calculated for each (x,y,z) position within the water phantom as:

$$k^{f_{clin},f_{ref}}_{Q_{clin},Q}(x,y,z) = \frac{\frac{D_{w,clinc}(x,y,z)}{D_{w,ref}(0,0,z_{ref})}}{\frac{D_{IC,clinic}(x,y,z)}{D_{IC,ref}(0,0,z_{ref})}} \quad (2)$$

In the following sections we describe Monte Carlo methods, models, experimental validation of results and type A and B uncertainty assessment.

Monte Carlo simulation

BEAMnrc code (Rev1.78 version) [24] was used to produce phase space files scored at the water phantom surface. These phase spaces were used in a next step as source to simulation of absorbed dose to air enclosed in ion chamber cavity and absorbed dose to a water voxel within a water phantom with egs_chamber code (version 1.21) [25].

The model of a 6FFF Varian TrueBeam described and validated in [23] was used in the present work to produce 6FFF fields. Same primary electron parameters found in that work were considered in this study.

Following same philosophy as described in [23], a detailed model of a 10FFF Varian TrueBeam was developed with the following two main differences respect to 6FFF model: the target was modified (the model consisted of a 0.65 mm thick tungsten sheet that rests on a 9.1 mm layer of copper) and a 1 mm thin brass slab was added after primary collimator. In order to obtain primary electron parameters of 10FFF model (mean energy and focal spot size), same procedure as described in [23] was used. 5 × 5, 10 × 10 and 20 cm × 20 cm fields were used for selecting beam model primary electron source parameters.

Clinical static field for both 6FFF and 10FFF commissioned beams considered was a BrainLab 5 mm diameter cone and reference field was a 3 cm × 3 cm field. Therefore, calculation of absorbed doses in equations (1) and (2) required simulating these same phase spaces for both beam modalities, which were scored at 92.5, 98, 98.5 or 100 cm from source depending on measurement to be corrected. Phase spaces are listed in Table 2. Jaw settings for the 3x3 fields were adjusted as to reproduce same exact field size as in measurements.

Simulation of absorbed dose to air inside ion chamber cavity was carried out with egs_chamber following the methods described in [23]. As it was shown in that previous work, accurate reproduction of experimental data requires simulation of detector response within geometry as close as possible to actual detector geometry. Detailed models of the chambers listed in Table 1 were implemented with egs++ combinatory geometry functions. Chamber reference points are placed on axis at a reference depth. Absorbed dose to water was simulated with egs_chamber with same transport parameters and Variance Reduction Techniques as in absorbed dose to air simulations. Absorbed dose to water was scored in a cubic voxel centred at same position as chamber reference point. Reference depths are listed in Table 2. Water voxel

Table 1
Ionization chambers considered in this work and summary of characteristics.

Manufacturer and model	Cavity Dimensions (radius/length, mm)	Active volume (cm^3)	Electrode materials (central/wall)
PTW T31022 Pinpoint	1.45/2.9	0.016	Aluminum/ Graphite, PMMA
IBA-dosimetry CC01	1/3.1	0.01	Steel/C552
Standard Imaging A16	1.27/2.46	0.007	Nickel-copper/ A150
IBA-dosimetry RAZOR Nano Chamber	1/*	0.003	Graphite/ Graphite
PTW T31010 Semiflex**		0.125	Aluminum/ Graphite, PMMA

*The cavity of this chamber is spherical.
**This chamber was used in Monte Carlo beam model commissioning; no correction factors are presented in this work.

Table 2
Source to surface distance and reference depth per measurement type and beam energy studied, and voxel dimensions in the corresponding absorbed dose to water Monte Carlo simulations.

Energy	Measurement	SSD (cm)	Reference depth (cm)	Water voxel dimensions (mm)
6FFF	Output Factor	100	5	0.2 × 0.2 × 1
10FFF	Output Factor	100	5	0.2 × 0.2 × 1
6FFF	5 mm cone beam profile	92.5	7.5	0.4 × 0.4 × 1
10FFF	5 mm cone beam profile	92.5	7.5	0.4 × 0.4 × 1
6FFF	5 mm cone PDD	98.5	–	0.8 × 0.8 × 0.5
10FFF	5 mm cone PDD	98	–	0.8 × 0.8 × 0.5

dimensions were adjusted to improve statistics without biasing simulation results and are listed in Table 2.

Experimental validation

Proper experimental validation of Monte Carlo simulation is essential for producing accurate results. In our approach, experimental validation of simulated correction factors was based on three tests, namely: i) checking beam model in wide fields; ii) checking chamber model in cone collimated fields and iii) checking output factor simulation:

Firstly, we checked that our beam model reproduced ionometric measurements of Percent Depth Doses (PDD) and beam profiles inside a water tank for wide fields between 5 × 5 and 20 cm × 20 cm within tolerances. Beam profiles were measured with a PTW T31022 Pinpoint ion chamber and PDDs with a PTW T31010 Semiflex ion chamber and simulated using air within cavities of models of these same detectors as scoring geometries. We established as pass criterion that all simulated points reproduced measured points within 1% of relative local deviation for PDD and 1% of relative deviation for beam profiles.

Secondly, we checked that our chamber models reproduced experimental percent depth doses and beam profiles for 5 mm cone collimated beams (6FFF and 10FFF) as measured by chambers within tolerances. Pass criterion was 1% of relative local deviation for PDD and 1% of relative deviation for beam profiles.

Finally, we simulated output factors for which corrections were to be calculated and compared them with measured output factors for all of the chambers studied. Pass criterion was 1% of relative local deviation.

Uncertainty

Monte Carlo simulation uncertainty

Monte Carlo simulation gives an estimate of type A uncertainty of averaged absorbed dose scored by individual particle tracks. This type A uncertainty can be propagated to correction factors calculated according to equations (1) or (2). However, other uncertainty contributions can only be estimated as type B and must be evaluated separately and added to propagated type A uncertainty.

If we consider correction factors as functions which depend on a set of parameters p_i (which can be scoring geometry position or phase space primary source parameters), then we can propagate type B uncertainty of the correction factor associated to type B uncertainty of parameters p_i by:

$$u\left(k_{Q_{clin},Q}^{f_{clin},f_{ref}}(p_i)\right)^2 = \sum_{i=1}^{n} u(p_i)^2 \left(\frac{\partial k_{Q_{clin},Q}^{f_{clin},f_{ref}}(p_i)}{\partial p_i}\right)^2 \approx$$

$$\approx \sum_{i=1}^{n} u(p_i)^2 \left(\frac{k_{Q_{clin},Q}^{f_{clin},f_{ref}}(p_i) - k_{Q_{clin},Q}^{f_{clin},f_{ref}}(p_i + u(p_i))}{u(p_i)}\right)^2 = \quad (3)$$

$$= \sum_{i=1}^{n} \left(k_{Q_{clin},Q}^{f_{clin},f_{ref}}(p_i) - k_{Q_{clin},Q}^{f_{clin},f_{ref}}(p_i + u(p_i))\right)^2$$

Two sources of type B uncertainty were considered:

- Positioning uncertainty: We considered 0.25 mm diagonal miss-positioning of the chamber within XY plane as worst case scenario. This value is large enough to contain contributions of miss-positioning of chamber respect to reference point and isocenter definition [26].
- Propagation of type B uncertainty of phase space primary source parameters. Uncertainties given by the commissioning procedure and shown in Table 3.

Therefore uncertainty in output factor correction factors is calculated according to:

$$\begin{aligned} u\left(k_{Q_{clin},Q}^{f_{clin},f_{ref}}\right)^2 = &\left(k_{Q_{clin},Q}^{f_{clin},f_{ref}}(E) - k_{Q_{clin},Q}^{f_{clin},f_{ref}}(E + u(E))\right)^2 \\ &+ \left(k_{Q_{clin},Q}^{f_{clin},f_{ref}}(FWHM) - k_{Q_{clin},Q}^{f_{clin},f_{ref}}(FWHM + u(FWHM))\right)^2 \\ &+ \left(k_{Q_{clin},Q}^{f_{clin},f_{ref}}(x_0, y_0) - k_{Q_{clin},Q}^{f_{clin},f_{ref}}(x_0 + u(x_0), y_0 + u(y_0))\right)^2 \\ &+ u\left(k_{Q_{clin},Q}^{f_{clin},f_{ref}}\right)^2_{typeA} \end{aligned} \quad (4)$$

Where: $u(E)$ and $u(FWHM)$ are uncertainties of beam model initial source energy and spatial FWHM, calculated as described in our previous work [13]; $u(x_0)$ and $u(y_0)$ are positioning uncertainties in × and y axis; $k_{Q_{clin},Q}^{f_{clin},f_{ref}}(E+u(E))$ is the correction factor evaluated for a beam with initial source energy $E + u(E)$; $k_{Q_{clin},Q}^{f_{clin},f_{ref}}(FWHM+u(FWHM))$ is the correction factor evaluated for a beam with initial source spatial distribution with a Full Width Half Maximum of $FWHM + u(FWHM)$; $k_{Q_{clin},Q}^{f_{clin},f_{ref}}(x_0+u(x_0), y_0+u(y_0))$ the correction factor evaluated at a position with coordinates $x_0+u(x_0)$ and $y_0+u(y_0)$ and $u\left(k_{Q_{clin},Q}^{f_{clin},f_{ref}}\right)^2_{typeA}$ is Monte Carlo estimated type A uncertainty. Similarly, uncertainties can be calculated in this way for position dependent correction factors as those calculated according to equation (2).

Experimental uncertainty

Following contributions to experimental uncertainty of ion chamber measurements were evaluated:

- Reproducibility of several consecutive measurements, without any geometrical changes.
- Reproducibility of measurements, after re-setting of whole geometry (water tank positioning, gantry setting, chamber positioning and collimator adjustment).

Results

Best values for primary electron mean energy and spot size and corresponding uncertainties were found after running the commissioning algorithm described in López-Sánchez et al. [23] through 10FFF measured and simulated data. These are shown in Table 3 together with parameters found in our previous work for 6FFF.

With these parameters, simulated and measured 10FFF PDDs and beam profiles of 5 × 5, 10 × 10 and 20 cm × 20 cm agreed within criteria defined in section ii.b except for a single point in the 10 cm × 10 cm field profile which exhibited 1.3% difference respect to its

Table 3
Beam model initial electron source parameters which best reproduce wide 6 and 10 FFF fields and associated uncertainties.

Beam Modality	MC Best Energy (MeV)	MC Best FWHM (mm)
6FFF	6.1 ± 0.1	1.60 ± 0.05
10FFF	10.4 ± 0.1	0.80 ± 0.05

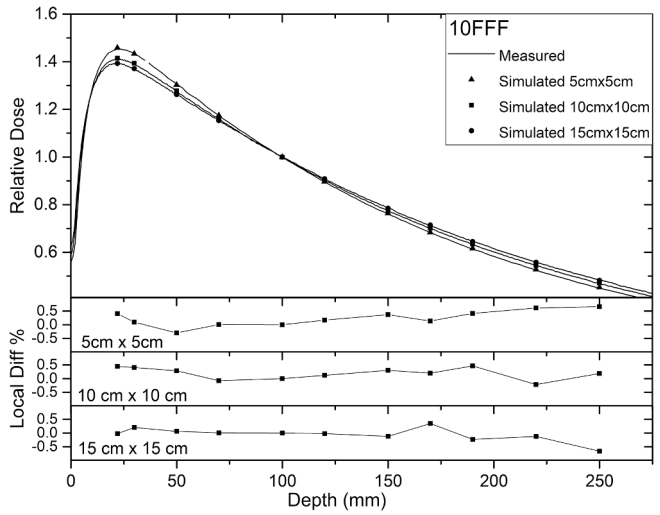

Fig. 1. Percent depth dose curves measured with a PTW T31010 Semiflex (continuous lines) and calculated within PTW T31010 Semiflex geometry by Monte Carlo simulation (triangles, squares and circles) for 5x5, 10x10 and 15 cm × 15 cm 10FFF fields. Relative Local differences between measured and simulated data are shown at bottom.

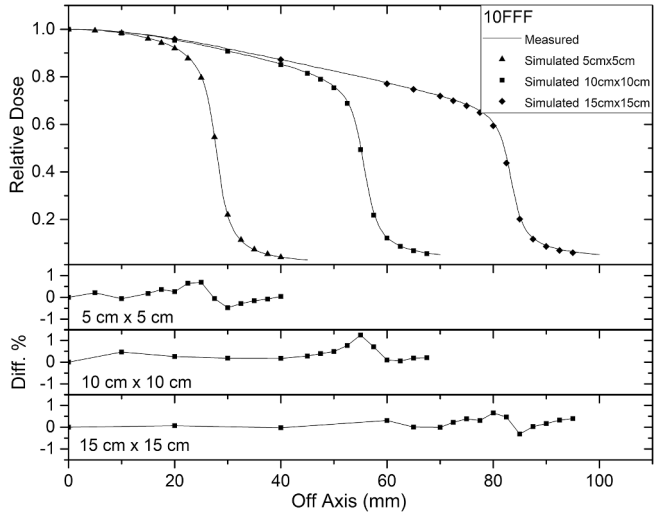

Fig. 2. Beam profile curves measured with a PTW T31022 Pinpoint (continuous lines) and calculated within PTW T31022 Pinpoint geometry by Monte Carlo simulation (triangles, squares and circles) for 5x5, 10x10 and 15 cm × 15 cm 10FFF fields. Relative differences between measured and simulated data are shown at bottom.

experimental value. This comparison is shown in Figs. 1 and 2.

After finding best simulation source parameters reproducing wide fields, we verified our beam models down to narrow beams (by inserting 5 mm Brainlab Cone collimation) and simultaneously we validated detector geometry models. Chamber cavity dimensions for all but IBA-dosimetry RAZOR Nano Chamber had to be adjusted within manufacturer tolerances in order to fit experimental data; these changes were supported by mammograph imaging of the chambers. These changes led to up to 2% variations in output factor.

Simulated absorbed dose to air enclosed in the cavity of modelled chambers reproduced experimental values of percent depth doses and beam profiles of 6FFF and 10FFF 5 mm cone collimated beams, measured with these chambers, within criteria defined in section ii.b except for 4 points of Razor Nano Chamber beam profile simulations: One in 6FFF and three in 10FFF 5 mm cone fields in which relative difference reached up to 1.5%. These results are shown in Fig. 3 and in Fig. 4 for the smallest and biggest active volume chambers considered in this study.

Finally, additionally to the correction factor results for small fields, we simulated output factors for all chambers and compared them with experimental data. All simulated output factors agreed with measurements within 1% relative local difference, as shown in Table 4. Output factor experimental uncertainty component associated with reproducibility ranged between 0.1% and 0.2%. Uncertainty component associated with geometry re-setting ranged between 0.2% and 0.4%. Both uncertainty components were minimum for PTW T31022 Pinpoint and maximum for IBA-dosimetry RAZOR Nano Chamber respectively.

6FFF and 10FFF 5 mm cone collimated output factor correction factors, calculated with equation (1) respect to a 3 cm × 3 cm reference field, for ion chambers considered in this study are shown in Table 5, with associated combined uncertainty, calculated itself with equation (4).

6 and 10 FFF 5 mm diameter field PDD and beam profile correction factors, calculated with expression (2), for PTW T31022 Pinpoint and IBA-dosimetry RAZOR Nano Chamber, are shown in Figs. 5 and 6.

Discussion

Agreement found between simulated and measured data validated our beam models and the election of primary electron beams for 10FFF for wide open fields, as it had been proved for 6FFF beam model in our previous work [23].

Agreement found between experimental and simulated cone field beam profiles and percent depth dose curves showed that chambers studied were correctly modelled in the simulations and further validated 6FFF and 10FFF beam models and primary electron source parameter election down to narrow fields.

Simulation result variations found in the fine tuning of chamber geometries were similar to what we have in our Secondary Standard Dosimetry Laboratory records for calibration coefficients in small active volume chambers. IBA-dosimetry RAZOR Nano Chamber nominal geometry was the only that did not require fine tuning of dimensions. This is normal since its cavity is much smaller than those of the other chambers and therefore fluence perturbation and volume averaging are minimal and do not affect output factor result.

It should be noted that our capacity to reproduce experimental results in simulations showed that our beam model is valid in general for all 6FFF and 10FFF TrueBeam units but that chamber models, other than IBA-dosimetry RAZOR Nano Chamber, are strictly valid only for the individual chamber units employed in our measurements, since we reproduced their particular geometry. Other chambers of same type may exhibit small manufacturing differences which may produce different responses.

As for output factor correction factors, PTW T31022 Pinpoint, the largest active volume chamber, exhibited the highest amount of correction. IBA-dosimetry CC01 and Standard Imaging Exradin A16 present both similar correction factors. All but one of the chambers studied need a correction higher than 5% in the 5 mm diameter field considered in this work. This makes them un-suitable for dosimetry in such a small field. Remarkably, however, IBA-dosimetry RAZOR Nano Chamber had a correction compatible with unity which makes it a suitable detector for small field output factor measurements. This follows the logical trend that the higher active volume, the higher volume averaging and therefore the higher correction factor. If a satisfactory evaluation on short and long term reproducibility is carried out, this chamber could be considered as a good candidate for reference dosimetry of small static fields.

Correction factor uncertainty was in general dominated by type B component associated with primary electron beam model FWHM uncertainty. This component decreases with active volume. As detector dimensions are reduced, on axis calculated response gets less sensitive to

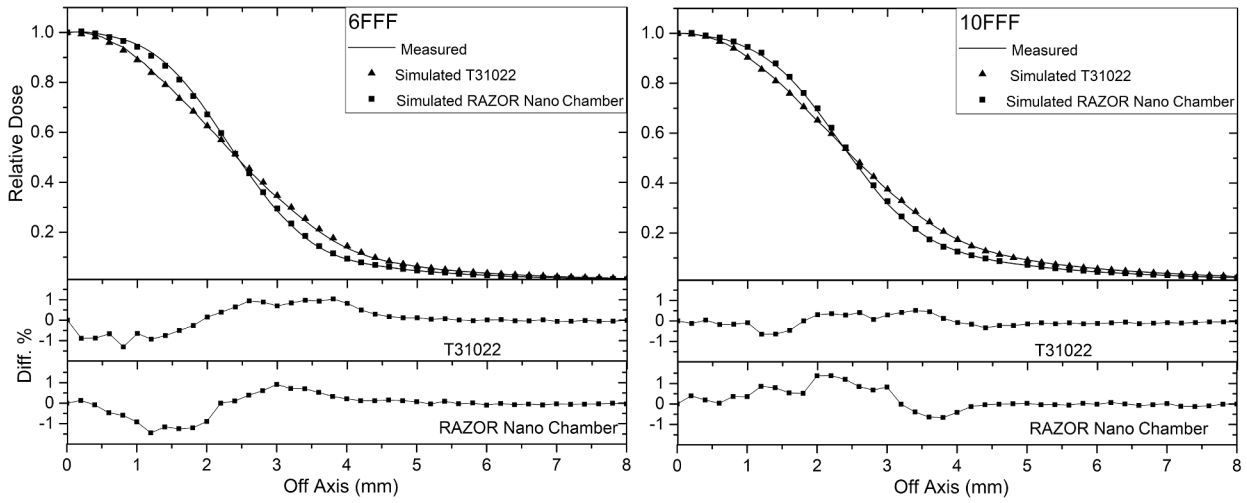

Fig. 3. Beam profile curves measured with PTW T31022 Pinpoint and IBA-dosimetry RAZOR Nano Chamber (continuous lines) and calculated within PTW T31022 Pinpoint and IBA-dosimetry RAZOR Nano Chamber geometries by Monte Carlo simulation (triangles and squares) for 6 FFF 5 mm cone field (left) and 10FFF 5 mm cone field (right). Relative differences between measured and simulated data are shown at bottom.

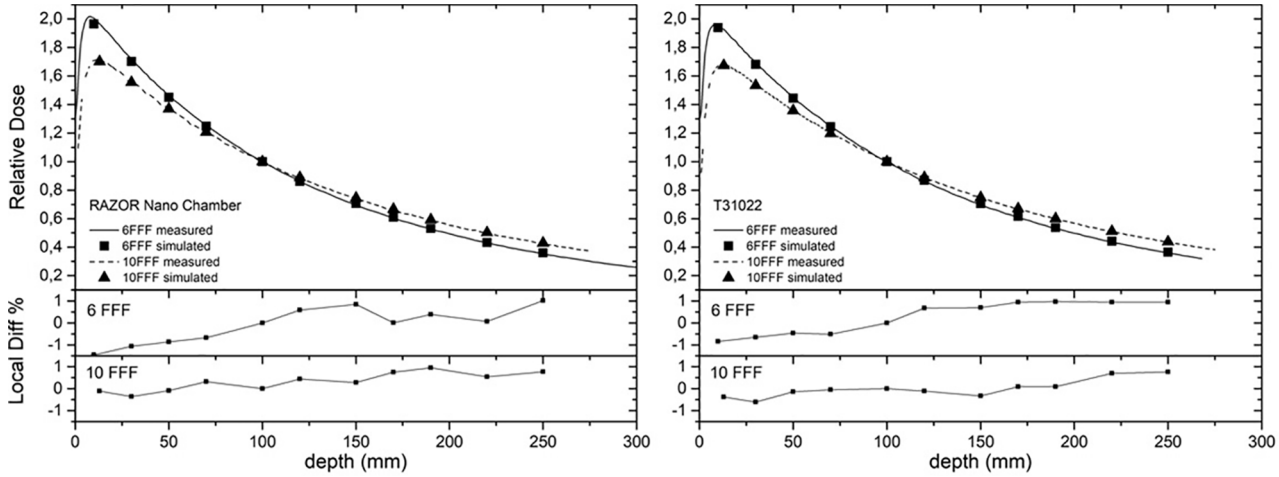

Fig. 4. Percent depth dose measured with chamber (lines) and calculated within chamber geometry by Monte Carlo simulation (symbols) for 6 FFF and 10 FFF 5 mm cone field. Left IBA-dosimetry RAZOR Nano Chamber and Right PTW T31022 Pinpoint. Relative Local differences between measured and simulated data are shown at bottom.

Table 4
Measured (exp OF) and simulated (MC OF) output factors for a 5 mm diameter collimator and for 6 FFF and 10 FFF beam modalities.

Chamber	6FFF 5 mm exp OF	6FFF 5 mm MC OF	Local relative difference	10FFF 5 mm exp OF	10FFF 5 mm MC OF	Local relative difference
PTW T31022 Pinpoint	0.623 ± 0.001	0.618 ± 0.005	−0.80%	0.524 ± 0.001	0.529 ± 0.004	0.95%
IBA-dosimetry CC01	0.637 ± 0.002	0.632 ± 0.006	−0.78%	0.543 ± 0.001	0.545 ± 0.004	0.33%
Standard Imaging Exradin A16	0.632 ± 0.002	0.629 ± 0.005	−0.60%	0.539 ± 0.002	0.542 ± 0.003	0.47%
IBA-dosimetry RAZOR Nano Chamber	0.685 ± 0.003	0.683 ± 0.004	−0.37%	0.587 ± 0.003	0.587 ± 0.002	0.01%

changes in beam profile induced by changes in FWHM. Type B component associated with positioning is minimal for the bigger and smaller active volume chambers and maximal for intermediate sized active volumes. This indicates that PTW T31022 Pinpoint correction is dominated by volume averaging and that cavity dimensions are comparable with beam size and therefore the correction is similar and large regardless of chamber miss positioning. On the other hand, IBA-dosimetry RAZOR Nano Chamber correction was always small (compatible with unity) as long as we consider miss-positioning within the nearly flat region of the beam. Intermediate active volume chambers are more sensitive to miss-positioning because they do not have a size comparable nor much smaller than with beam size. Type B uncertainty associated with beam model initial electron energy did not show any clear trend but IBA razor values were slightly higher than the rest, maybe due to composition of central electrode. Type B uncertainty associated with beam model parameter FWHM was minimal for smallest active volume and maximal for highest active volume, as an increase in FWHM broadens field penumbra and increases high volume chamber miss response [27]. As for combined uncertainty, IBA-dosimetry RAZOR Nano Chamber exhibited the lowest value since it presents a much

Table 5
6 and 10 FFF 5 mm cone field correction factors, calculated using equation (1) respect to a 3 cm × 3 cm reference field, and associated combined uncertainty for 4 ion chamber models considered in this work. Each uncertainty component is calculated as each of the bracketed terms of equation (4).

Chamber	Beam	$k_{Qclin,Q}^{fclin,fref}$	Type A uncert.	Type B uncert. (positioning)	Type B uncert. (E)	Type B uncert. (FWHM)	Combined Uncertainty
PTW T31022 Pinpoint	6FFF	1.107	0.004	0.001	0.002	0.007	0.008
	10FFF	1.111	0.004	0.001	0.004	0.006	0.008
IBA-dosimetry CC01	6FFF	1.084	0.004	0.005	0.006	0.006	0.010
	10FFF	1.077	0.004	0.007	0.005	0.005	0.010
Standard Imaging Exradin A16	6FFF	1.090	0.004	0.004	0.004	0.006	0.009
	10FFF	1.084	0.004	0.002	0.003	0.005	0.007
IBA-dosimetry RAZOR Nano Chamber	6FFF	1.005	0.005	0.002	0.004	0.002	0.007
	10FFF	1.002	0.004	0.001	0.002	0.004	0.006

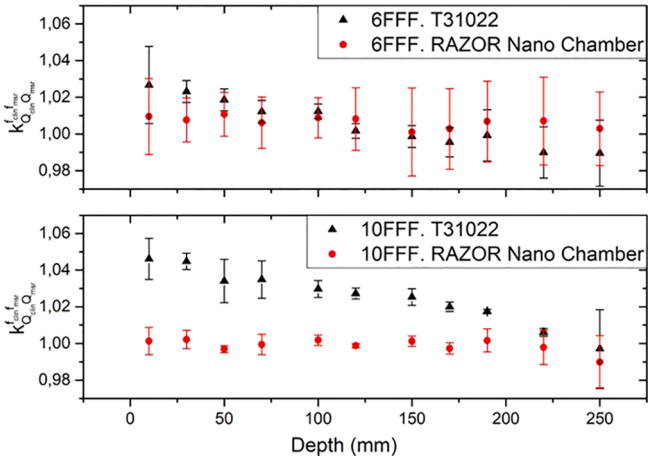

Fig. 5. Correction factor for 6 (top) and 10 FFF (bottom) 5 mm diameter field for PTW T31022 Pinpoint (black triangles) and IBA-dosimetry RAZOR Nano Chamber (red circles) as a function of depth.

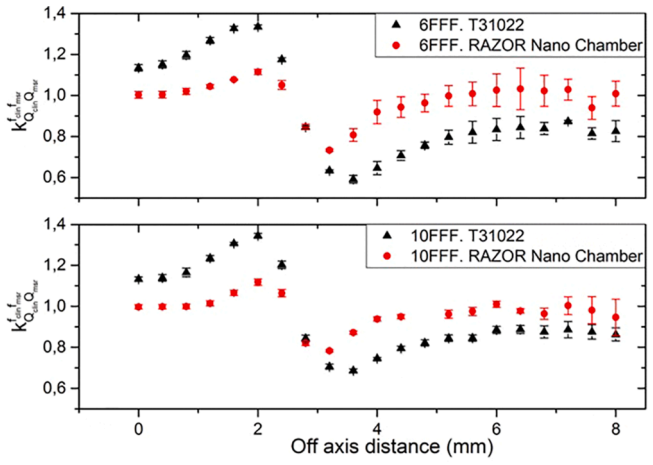

Fig. 6. Correction factor for 6 (top) and 10 FFF (bottom) 5 mm diameter field for PTW T31022 Pinpoint (black triangles) and IBA-dosimetry RAZOR Nano Chamber (red circles) as a function of Off Axis Distance.

smaller correction factor.

Percent depth dose correction factor results indicated that IBA-dosimetry RAZOR Nano Chamber can be used for small field percent depth dose measurements within 1% accuracy while PTW T31022 Pinpoint produces a miss response of up to 5% gradually decreasing with depth in water. As in output factor measurement, the combination of small active volume and small fluence perturbation is the reason for the adequate dosimetric behaviour of IBA-dosimetry RAZOR Nano Chamber.

As for beam profiles, calculated corrections showed that IBA-dosimetry RAZOR Nano Chamber produces a negligible volume averaging and fluence perturbation in the vicinity of beam axis, up to 1 mm of axis distance, which makes the chamber less prone to miss positioning errors while measuring output factors. Nevertheless, none of the chambers are suitable for 5 mm small field profile measurements given that most of measuring points fall within beam penumbra region.

Generic correction factors should be used with care since chamber to chamber variations could imply that different correction factors are needed. In other words, if manufacturing differences between chambers of the same model exist, then measured output factors could be different and therefore our chamber model geometries should be changed accordingly to yield valid correction factor results. Moreover, reference field size could be slightly different and produce a slightly different output factor. A reader looking for correction factors, before using data from this work, should measure output factors and compare them with experimental results shown in previous section.

Conclusions

We found that of the commercially available small active volume ion chambers studied, IBA-dosimetry RAZOR Nano Chamber, presents an output factor correction factor compatible with unity and also the lowest uncertainty when measuring 5 mm diameter 6 and 10 FFF fields. It can also be used to measure 5 mm diameter field percent depth doses within 1% accuracy and is insensitive up to +/- 1 mm miss positioning while measuring on axis output factors. The main conclusion of this work is, therefore, that this detector is an excellent choice for small field dosimetry since it presents all the advantages of an ion chamber over other detection technologies. This is caused by its excellent design, which on one hand produces minimum fluence perturbation because of its tiny active volume and its wall and electrode water equivalence and also because of its minimum volume averaging due again to its tiny active volume.

The authors insist in the fact that results presented here are self-consistent with the set of measurements of this work. Small detector to detector manufacturing differences, if exist, could produce different output factors and therefore require different corrections. A note of caution should be observed when using Monte Carlo calculated correction factors in generic geometries since that equates to considering generic calibration coefficients for a certain chamber type. A more accurate approach would be to consider type B uncertainty contributions to correction factors which take into account manufacturing differences.

Declaration of Competing Interest

The authors declare that they have no known competing financial interests or personal relationships that could have appeared to influence the work reported in this paper.

References

[1] Alfonso R, Andreo P, Capote R, Christaki K, Huq MS, Izewska J, et al. Dosimetry of small static fields used in external beam radiotherapy 2017;no. 483.

[2] Martens C, De Wagter C, De Neve W. The value of the PinPoint ion chamber for characterization of small field segments used in intensity-modulated radiotherapy. Phys Med Biol 2000;45:2519–30. https://doi.org/10.1088/0031-9155/45/9/306.

[3] Stasi M, Baiotto B, Barboni G, Scielzo G. The behavior of several microionization chambers in small intensity modulated radiotherapy fields. Med Phys 2004;31(10):2792–5. https://doi.org/10.1118/1.1788911.

[4] Capote R, Sánchez-Doblado F, Leal A, Lagares JI, Arráns R, Hartmann GH. An EGSnrc Monte Carlo study of the microionization chamber for reference dosimetry of narrow irregular IMRT beamlets. Med Phys 2004;31(9):2416–22.

[5] Agostinelli S, Garelli S, Piergentili M, Foppiano F. Response to high-energy photons of PTW31014 PinPoint ion chamber with a central aluminum electrode. Med Phys 2008;35(7Part1):3293–301.

[6] Miller JR, Hooten BD, Micka JA, DeWerd LA. Polarity effects and apparent ion recombination in microionization chambers. Med Phys 2016;43(5):2141–52. https://doi.org/10.1118/1.4944872.

[7] De Angelis C, Onori S, Pacilio M, Cirrone GAP, Cuttone G, Raffaele L, et al. An investigation of the operating characteristics of two PTW diamond detectors in photon and electron beams. Med Phys 2002;29(2):248–54.

[8] Ciancaglioni I, Marinelli M, Milani E, Prestopino G, Verona C, Verona-Rinati G, et al. Dosimetric characterization of a synthetic single crystal diamond detector in clinical radiation therapy small photon beams: dosimetric characterization of a synthetic single crystal diamond detector. Med Phys 2012;39(7Part1):4493–501.

[9] Lárraga-Gutiérrez JM, Ballesteros-Zebadúa P, Rodríguez-Ponce M, García-Garduño OA, de la Cruz OOG. Properties of a commercial PTW-60019 synthetic diamond detector for the dosimetry of small radiotherapy beams. Phys Med Biol 2015;60(2):905–24.

[10] Gómez-Rodríguez F, Gonzalez-Castaño DM, Gómez Fernández N, Pardo-Montero J, Schüller, A, Gasparini A, Vanreusel V, Verellen D, Felici G, Kranzer R, Paz-Martín J. Development of an Ultra-Thin Parallel Plate Ionization Chamber for Dosimetry in FLASH Radiotherapy. Med. Phys. *In Press*.

[11] De Martin E, Alhujaili S, Fumagalli ML, Ghielmetti F, Marchetti M, Gallo P, et al. On the evaluation of edgeless diode detectors for patient-specific QA in high-dose stereotactic radiosurgery. Phys Med 2021;89:20–8. https://doi.org/10.1016/j.ejmp.2021.07.010.

[12] De Coste V, Francescon P, Marinelli M, Masi L, Paganini L, Pimpinella M, Prestopino G, Russo S, Stravato A, Verona C, Verona-Rinati G. Is the PTW 60019 microDiamond a suitable candidate for small field reference dosimetry? Phys Med Biol 2017;62:7036–55. https://doi.org/10.1088/1361-6560/aa7e59.

[13] Andreo P, Palmans H, Marteinsdóttir M, Benmakhlouf H, Carlsson-Tedgren Å. On the Monte Carlo simulation of small-field micro-diamond detectors for megavoltage photon dosimetry. Phys Med Biol 2016;61(1):L1–10.

[14] Hartmann G, Zink K. A Monte Carlo study on the PTW 60019 microDiamond detector. Med Phys 2019;46(11):5159–72. https://doi.org/10.1002/mp.13721.

[15] Marinelli M, Prestopino G, Verona C, Verona-Rinati G. Experimental determination of the PTW 60019 microDiamond dosimeter active area and volume. Med Phys 2016;43(9):5205–12. https://doi.org/10.1118/1.4961402.

[16] Butler DJ, Beveridge T, Lehmann J, Oliver CP, Stevenson AW, Livingstone J. Spatial response of synthetic microDiamond and diode detectors measured with kilovoltage synchrotron radiation. Med Phys 2018;45(2):943–52.

[17] Russo S, Reggiori G, Cagni E, Clemente S, Esposito M, Falco MD, et al. Small field output factors evaluation with a microDiamond detector over 30 Italian centers. Physica Med 2016;32(12):1644–50.

[18] Casar B, Gershkevitsh E, Mendez I, Jurković S, Saiful Huq M. Output correction factors for small static fields in megavoltage photon beams for seven ionization chambers in two orientations — perpendicular and parallel. Med Phys 2020;47(1):242–59. https://doi.org/10.1002/mp.13894.

[19] Partanen M, Niemelä J, Ojala J, Keyriläinen J, Kapanen M. Properties of IBA Razor Nano Chamber in small-field radiation therapy using 6 MV FF, 6 MV FFF, and 10 MV FFF photon beams. Acta Oncol 2021:1–6. https://doi.org/10.1080/0284186X.2021.1979644.

[20] Looe HK, Büsing I, Tekin T, Brant A, Delfs B, Poppinga D, et al. The polarity effect of compact ionization chambers used for small field dosimetry. Med Phys 2018;45(12):5608–21.

[21] Falco MD, Fusella M, Clemente S, Fiandra C, Gallio E, Garibaldi C, et al. The influence of basic plan parameters on calculated small field output factors – A multicenter study. Physica Med 2021;88:98–103.

[22] Dufreneix S, Bellec J, Josset S, Vieillevigne L. Field output factors for small fields: a large multicenter study. Phys Med 2021;81:191–6. https://doi.org/10.1016/j.ejmp.2021.01.001.

[23] López-Sánchez M, Pérez-Fernández M, Fandiño JM, Teijeiro A, Luna-Vega V, Gómez-Fernández N, et al. An EGS Monte Carlo model for Varian TrueBEAM treatment units: commissioning and experimental validation of source parameters. Phys Med 2019;64:81–8. https://doi.org/10.1016/j.ejmp.2019.06.017.

[24] Rogers DWO, Faddegon BA, Ding GX, Ma CM, Wei J, Mackie TR. BEAM: a Monte Carlo code to simulate radiotherapy treatment units. Med Phys 1995;22:503–24. https://doi.org/10.1118/1.597552.

[25] Wulff J, Zink K, Kawrakow I. Efficiency improvements for ion chamber calculations in high energy photon beams. Med Phys 2008;35(4):1328–36. https://doi.org/10.1118/1.2874554.

[26] Francescon P, Beddar S, Satariano N, Das IJ. Variation of kQclin, Qmsrfclin, fmsr for the small-field dosimetric parameters percentage depth dose, tissue-maximum ratio, and off-axis ratio. Med Phys 2014;41(10):101708.

[27] González-Castaño D, Pena J, Sánchez-Doblado F, Hartmann GH, Gómez F, Leal A. The change of response of ionization chambers in the penumbra and transmission regions: impact for IMRT verification. Med Biol Eng Comput 2008;46(4):373–80. https://doi.org/10.1007/s11517-007-0249-z.